

# Hydrothermal synthesis of LiFePO<sub>4</sub> nanorods composed of nanoparticles from vivianite precursor and its electrochemical performance for lithium ion battery applications

S RAGHUPATI RAO and U V VARADARAJU\*

Department of Chemistry, Indian Institute of Technology Madras, Chennai 600 036, India

MS received 21 May 2014; accepted 7 April 2015

**Abstract.** LiFePO<sub>4</sub> nanorods composed of nanoparticles were synthesized from precursor phase Fe<sub>3</sub>(PO<sub>4</sub>)<sub>2</sub>(H<sub>2</sub>O)<sub>8</sub> (vivianite) via hydrothermal reaction. Nanorods consisting of nanoparticles were formed by using L-(+)-ascorbic acid as reducing and capping agent. Near-theoretical specific capacity is achieved at 0.1 C rate with excellent retention capacity of up to 50 cycles. Morphology of as-synthesized samples favours fast intercalation/deintercalation process with easy mass and charge transfer.

**Keywords.** Nanostructures; solvothermal; electron microscopy; electrochemical properties.

## 1. Introduction

LiFePO<sub>4</sub> is a promising cathode material with ordered olivine structure; belongs to Pnma space group. Padhi *et al.*,<sup>1</sup> pioneers of LiFePO<sub>4</sub> material, reported 0.6 Li insertion/deinsertion per formula unit by electrochemically. Since then several research groups explored LiFePO<sub>4</sub> as a cathode material with improved electrochemical properties. The compound exhibits a plateau behaviour in the voltage–composition profile at 3.45 V vs. Li<sup>+</sup>/Li<sup>0</sup>. The theoretical specific capacity is 170 mAh g<sup>-1</sup>. The voltage window of this material is well within the operation window of polymer and carbonate electrolytes.<sup>2,3</sup> The presence of iron in the compound makes LiFePO<sub>4</sub> an inexpensive and environmentally benign material for commercial applications. It also has an excellent thermal and chemical stability. The delithiated FePO<sub>4</sub> has essentially same structure as LiFePO<sub>4</sub>.<sup>4</sup> Delithiation (charging) results in 6.81% decrease in volume and 2.59% increase in density. The structural similarity between LiFePO<sub>4</sub> and FePO<sub>4</sub> mitigates capacity degradation during cycling process as well as largely compensates volume changes in graphite anode. This makes cycling capability of LiFePO<sub>4</sub> better than that of other oxide materials exhibiting excellent capacity retention even after couple of thousands of cycles.<sup>5</sup>

LiFePO<sub>4</sub> has one-dimensional (1D) channel along the *b*-axis; these 1D channels can be blocked by foreign phases, by stacking faults or by ionic disorder. In addition, low intrinsic electronic conductivity (10<sup>-9</sup> S cm<sup>-1</sup>) of LiFePO<sub>4</sub> has hindered its large-scale commercialization.<sup>6,7</sup> Synthesis conditions play crucial role on its electrochemical properties. Insufficient reducing conditions during synthesis

may leave Fe<sup>3+</sup> impurities. Nanophases are more promising than bulk material for better electrochemical performance, since larger particles contain stacking faults. As there is less ionic disorder in LiFePO<sub>4</sub>, it will not affect its electrochemical performance significantly. Nanophases of LiFePO<sub>4</sub> with controlled morphology are proven to show high rate capability with excellent retention capacity even after couple of thousands of cycles. Among the various synthesis techniques available, the hydrothermal route is found to be economically viable.<sup>8</sup>

Availability of a wide range of precursors, surfactants or morphology directing agents and reducing agents usage in hydrothermal synthesis process gives flexibility to synthesize nano-LiFePO<sub>4</sub> phases with different morphologies. These factors made the hydrothermal synthesis route inexpensive for the synthesis of commercial LiFePO<sub>4</sub> nanophases with controlled morphology at lower temperatures (~200°C) in a short period of time.<sup>9–11</sup> During hydrothermal process with precursors FeSO<sub>4</sub>·7H<sub>2</sub>O, NH<sub>4</sub>H<sub>2</sub>PO<sub>4</sub> and LiOH, Fe<sub>3</sub>(PO<sub>4</sub>)<sub>2</sub>(H<sub>2</sub>O)<sub>8</sub> (vivianite) is formed as an intermediate. It reacts with LiOH and results in the formation of final product. In the present work, we have synthesized LiFePO<sub>4</sub> nanorods from Fe<sub>3</sub>(PO<sub>4</sub>)<sub>2</sub>(H<sub>2</sub>O)<sub>8</sub> (vivianite) precursor via the hydrothermal route using L-(+)-ascorbic acid as a reducing and capping agent<sup>12</sup> for the first time.

## 2. Experimental

### 2.1 Synthesis

LiFePO<sub>4</sub> nanorods are synthesized by the hydrothermal route with Fe<sub>3</sub>(PO<sub>4</sub>)<sub>2</sub>(H<sub>2</sub>O)<sub>8</sub> (vivianite) as a precursor.

\*Author for correspondence (varada@iitmadras.ac.in)

Vivianite is synthesized via the hydrothermal route by using  $\text{FeSO}_4 \cdot 7\text{H}_2\text{O}$  ( $\geq 99.0\%$ , Rankem),  $\text{NH}_4\text{H}_2\text{PO}_4$  ( $\geq 98.5\%$ , Merck) as precursors. To a 0.1 M  $\text{FeSO}_4 \cdot 7\text{H}_2\text{O}$  (30.0 ml) solution, 0.13 M  $\text{NH}_4\text{H}_2\text{PO}_4$  (30.0 ml) solution is added in a 90 ml Teflon-lined autoclave and heated at  $60^\circ\text{C}$  for 24 h. The obtained product was washed with ethanol and de-ionized water for several times and dried in vacuum oven at  $60^\circ\text{C}$  for 3 h.<sup>13</sup> Stoichiometric amount of vivianite is added to 15.0 ml of distilled water to prepare vivianite suspension.

$\text{LiFePO}_4$  was synthesized from vivianite and  $\text{LiOH} \cdot \text{H}_2\text{O}$  ( $\geq 99.0\%$ , SRL) via the hydrothermal route for the first time. To the 0.1 M vivianite suspension (15 ml), 0.3 M  $\text{LiOH} \cdot \text{H}_2\text{O}$  (15 ml) and 0.1 M L-(+)-ascorbic acid (99% Aldrich) (3.5 ml) was added as an *in-situ* reducing agent in a 50 ml Teflon-lined autoclave and heated at  $180^\circ\text{C}$  for 6 h.<sup>14,15</sup> The obtained product was washed with ethanol and de-ionized water for several times and dried in vacuum oven at  $60^\circ\text{C}$  for 3 h.

## 2.2 Structural characterization and electrochemical studies

Phase purity was checked by powder X-ray diffraction (XRD) employing a scan speed of  $0.02^\circ$  per second in the  $2\theta$  range from  $10^\circ$  to  $80^\circ$  using a D8 Bruker X-ray diffractometer equipped with  $\text{Cu-K}\alpha$  radiation. The accelerating voltage and current was 40 kV and 40 mA, respectively. Morphology and size of all samples were measured by scanning electron microscopy (SEM) with a HITACHI S-4800 field-emission scanning electron microscope (FESEM) operated at 10 kV and 10 mA.

For electrochemical evaluation, slurry is made up of 70 wt%  $\text{LiFePO}_4$ , 20 wt% carbon black and 10 wt% polyvinylidene difluoride (PVDF) using N-methyl 2-pyrrolidone as solvent. The weighed materials were ground homogeneously and the resulting slurry was coated on stainless steel foils and dried in hot air oven over night at  $60^\circ\text{C}$ . The weight of the active material was found to be around 3–6 mg on each electrode. Electrochemical studies were performed in Swagelok-type cells. The cells were assembled in an argon-filled glove box (labstar, Mbraun, Germany). An electrochemical model cell was constructed using cathode, anode (Li metal), 1 M  $\text{LiPF}_6$  solution in ethylene carbonate–dimethyl carbonate (1 : 1 in volume) as the electrolyte (Chiel Industries Ltd., Korea) and a borosilicate glass fibre sheet as the separator. The cells were galvanostatically charged and discharged between the 3.0–3.7 V window vs.  $\text{Li}^+/\text{Li}^0$  at room temperature ( $25^\circ\text{C}$ ) on computer-controlled electrochemical analyzer (Model BT2000, Arbin Instruments, USA). Specific capacities were calculated based on the mass of active material.

## 3. Results and discussion

### 3.1 Microstructural studies

SEM images of as-synthesized  $\text{LiFePO}_4$  are shown in figure 1. Nanorod morphology is observed uniformly for  $\text{LiFePO}_4$ . On further magnification, these nanorods were found to be composed of nanoparticles. The dimensions of average particle size of as-synthesized nanorods are shown in figure 3b. The nanorods are typically 340 nm in length and 100 nm in width. It is known that in nano- $\text{LiFePO}_4$  with platelet morphology, the Li channels are oriented parallel to the short dimension, i.e., along the *b*-axis.<sup>16</sup> From the SEM images we emphasize that the diffusion path lengths for Li ions are on an average of 100 nm along the *b*-direction. Powder XRD patterns of  $\text{Fe}_3(\text{PO}_4)_2(\text{H}_2\text{O})_8$  (vivianite) and  $\text{LiFePO}_4$  are shown in supplementary figures S1 and S2, respectively. All peaks indexed with the monoclinic and orthorhombic space groups, respectively, indicating that both are single phase materials. Vivianite crystallizes in monoclinic crystal system with space group  $\text{C12/m1}$  and  $\text{LiFePO}_4$  crystallizes in orthorhombic crystal system with  $\text{Pnma}$  space group. The lattice parameters and

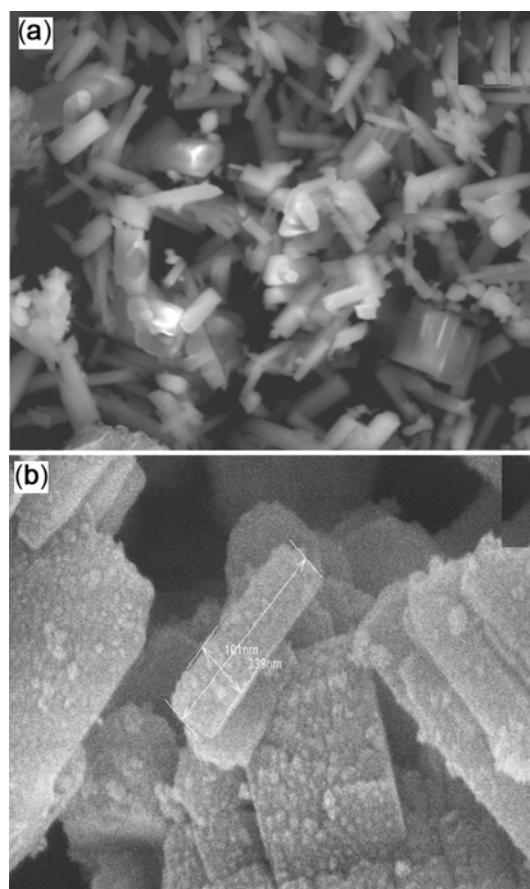
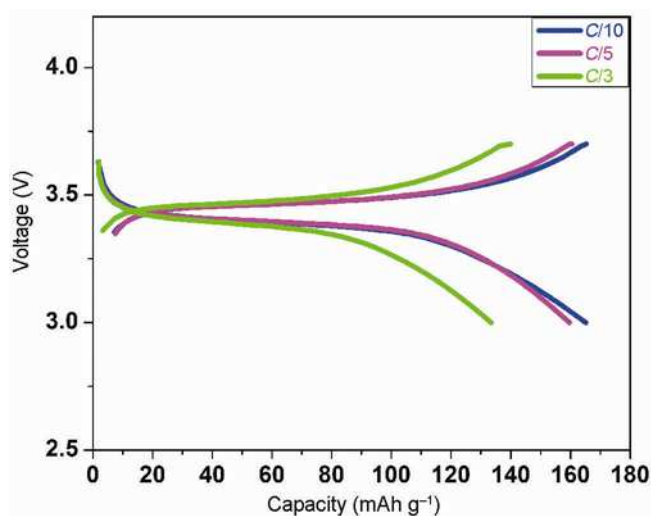


Figure 1. SEM images of the synthesized  $\text{LiFePO}_4$ .



**Figure 2.** Charge–discharge profiles of first cycles at different current densities.

$\alpha$ -,  $\beta$ -,  $\gamma$ -values shown in figures match well with those reported in the literature.<sup>17,18</sup>

### 3.2 Electrochemical charge–discharge studies

First charge–discharge profiles and cycling performance of as-synthesized samples with different  $C$  rates (0.1 $C$ , 0.2 $C$  and  $C/3$ ) are shown in figures 2 and 3, respectively. Charge and discharge capacities of  $\text{LiFePO}_4$  are same at 0.1 $C$  and 0.2 $C$  rates. It shows a capacity of 165, 160  $\text{mAh g}^{-1}$  at 0.1 $C$  and 0.2 $C$  rates, respectively, at an average voltage of 3.45 V vs.  $\text{Li}^+/\text{Li}^0$ . Whereas at  $C/3$  rate, charge capacity of 140  $\text{mAh g}^{-1}$  and discharge capacity of 135  $\text{mAh g}^{-1}$  at average voltage of 3.45 V vs.  $\text{Li}^+/\text{Li}^0$  are observed. At  $C/3$  rate charge capacity values are little higher than discharge capacity for first few cycles. There is almost 100% capacity retention up to 50 cycles at 0.1 $C$  and 0.2 $C$  rates. Good rate capability and capacity retention of this material can be explained on the basis of the morphology of the sample. The morphology of as-synthesized samples in the present study is nanorods, which in turn are composed of nanoparticles leading to shorter diffusion path lengths for lithium. According to domino cascade model<sup>16</sup> at a given point of time the  $\text{LiFePO}_4$  particle either should be completely discharged or charged. This means at a given point of time nanoparticles in nanorods also will be completely charged or discharged. In addition to that, shorter dimension of  $\sim 100$  nm in nanorods and nanoparticles in nanorods contributes to faster lithium intercalation/deintercalation process. The polarization could be due to the absence of conducting additive in the sample during synthesis. Electrochemical charge–discharge studies of  $\text{LiFePO}_4$  with conductive additives such as carbon nanotube, reduced

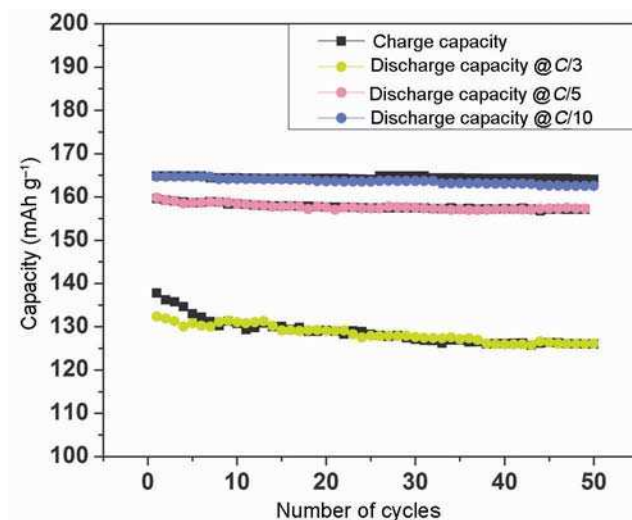


**Figure 3.** Cycling performance of  $\text{LiFePO}_4$  at different current densities.

graphene oxide and carbon coating with excess of ascorbic acid are underway to minimize the polarization at high  $C$  rates.

## 4. Conclusions

In conclusion, we have synthesized  $\text{LiFePO}_4$  nanorods composed of nanoparticles by a new hydrothermal synthesis method from  $\text{Fe}_3(\text{PO}_4)_2(\text{H}_2\text{O})_8$  (vivianite) precursor within 6 h without further heat treatment. Near-theoretical capacities are achieved at 0.1 $C$  rate with excellent capacity retention even up to 50 cycles. The phase shows initial capacity of 140  $\text{mAh g}^{-1}$  and a capacity of 130  $\text{mAh g}^{-1}$  after 50 cycles at  $C/3$  rate. The nanorods composed of nanoparticles provided shorter diffusion paths for lithium intercalation, which greatly improves the lithium storage capacity at good  $C$  rates and its cycling performance.

### Electronic supplementary material

Supplementary material pertaining to this article is available on the Bulletin of Materials Science website ([www.ias.ac.in/matensci](http://www.ias.ac.in/matensci)).

## References

1. Padhi A K, Nanjundaswamy K S and Goodenough J B 1997 *J. Electrochem. Soc.* **144** 1188
2. Padhi A K, Nanjundaswamy K S, Masquelier C, Okada S and Goodenough J B 1997 *J. Electrochem. Soc.* **144** 1609
3. Yamada A, Chung S C and Hinokuma K 2001 *J. Electrochem. Soc.* **148** A224
4. Andersson A S and Thomas J O 2001 *J. Power Sources* **97–98** 498

5. Wang Y, Wang Y, Hosono E, Wang K and Zhou H 2008 *Angew. Chem. Int. Ed.* **47** 7461
6. Franger S, Cras F L, Bourbon C and Rouault H 2002 *Electrochem. Solid-State Lett.* **5** A231
7. Prosini P, Lisi M, Zane D and Pasquali M 2002 *Solid State Ion.* **148** 45
8. Delacourt C, Poizot P, Tarascon J M and Masquelier C 2005 *Nat. Mater.* **4** 254
9. Whittingham M S 2004 *Chem. Rev.* **104** 4271
10. Ni J, Morishita M, Kawabe Y, Watada M, Takeichi N and Sakai T 2010 *J. Power Sources* **195** 2877
11. Dokko K, Koizumi S, Nakano H and Kanamura K 2007 *J. Mater. Chem.* **17** 4803
12. Hiroaki U and Hiroaki I 2010 *Cryst. Growth Des.* **10** 1777
13. Mattievich E and Danon J 1977 *J. Inorg. Nucl. Chem.* **39** 569
14. Chen C, Liu G B, Wang Y, Li J L and Liu H 2013 *Electrochim. Acta* **113** 464
15. Raghupati Rao S and Varadaraju U V 2013 In *International conference on materials for advanced technologies (ICMAT2013), symposium A* (Singapore) p A-PO1-67
16. Delmas C, Maccario M, Croguennec L, Cras F L and Weill F 2008 *Nat. Mater.* **7** 665
17. Gasperin M, Poullen J F and Fejdi P 1980 *Bull. Mineral.* **103** 135
18. Thomas J O, Haeggstroem L, Kalska B and Andersson A S 2000 *Solid State Ion.* **130** 41